

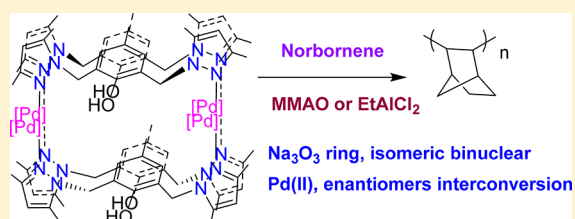
Enantiomers and Structural Isomers of Sodium and Palladium Complexes Bearing *ortho*-Bis(3,5-dimethylpyrazolylmethyl)phenolate: Fluxional Property and Highly Active Catalysts for Norbornene Polymerization

 Oishi Jana and Ganesan Mani*[✉]

Department of Chemistry, Indian Institute of Technology, Kharagpur, West Bengal 721 302, India

Supporting Information

ABSTRACT: 2,6-Bis(3,5-dimethylpyrazolylmethyl)-4-methylphenol **LH** was readily synthesized by the reaction between 2,6-bis-[(dimethylamino)methyl]-4-methylphenol and 3,5-dimethylpyrazole. The X-ray structure of the trisodium complex of **LH** showed the benzene-like planar Na_3O_3 ring with alternative shorter (2.181–2.185 Å) and longer (2.244–2.263 Å) bonds. The reaction of anionic ligand **L** with $[\text{PdCl}_2(\text{COD})]$ yielded three Pd(II) complexes: $[\text{Pd}\{\text{OC}_6\text{H}_2(\text{CH}_2\text{Pz}^{\text{Me}_2})_{2-2,6-\text{Me}-4-\kappa\text{N},\text{O}}\}_2]$ (**1**), $[\text{PdCl}\{\mu\text{-OC}_6\text{H}_2(\text{CH}_2\text{Pz}^{\text{Me}_2})_{2-2,6-\text{Me}-4-\kappa\text{N},\text{O},\text{N}}\}_2]$ (**2**), and $[\text{PdCl}_2\{\mu\text{-OC}_6\text{H}_2(\text{CH}_2\text{Pz}^{\text{Me}_2})_{2-2,6-\text{Me}-4-\kappa\text{N},\text{O},\text{N}}\}_2\text{Pd}]$ (**3**) (Pz^{Me_2} = 3,5-dimethylpyrazole). Conversely, the neutral ligand **LH** reacts with $[\text{PdCl}_2(\text{PhCN})_2]$ to give the 20-membered palladacycle, $[\text{Pd}_2\text{Cl}_4\{\mu\text{-HOC}_6\text{H}_2(\text{CH}_2\text{Pz}^{\text{Me}_2})_{2-2,6-\text{Me}-4-\kappa\text{N},\text{N}}\}_2]$ (**4**). **2** and **3** are structural isomers and rigid molecules, whereas **1** and **4** are fluxional, as shown by their ^1H NMR spectra. Hence, the dynamic behaviors of **1** and **4** were studied by variable-temperature ^1H NMR methods and are proposed to be interconversion processes: cis–trans for **1** and two chiral enantiomers for **4**. The structures of all complexes were determined by single crystal X-ray diffraction methods, which showed the presence of two different conformations of **LH** (trans and semitrans) bound to metal atoms. In addition, complexes **2–4** were found to be excellent precatalysts for the vinyl polymerization of norbornene in the presence of varying amount of MMAO and EtAlCl_2 in toluene or CH_2Cl_2 . Within a short period of time (1 min), almost all monomers are changed to polymers with one micromole of precatalyst. The optimized conditions of 1000 molar excess of MMAO gave 1.20×10^8 g PNB $\text{mol}^{-1} \text{h}^{-1}$ at room temperature. These addition polymers are completely insoluble in several organic solvents and hence were only characterized by ^1H , IR, powder XRD, and TGA methods.



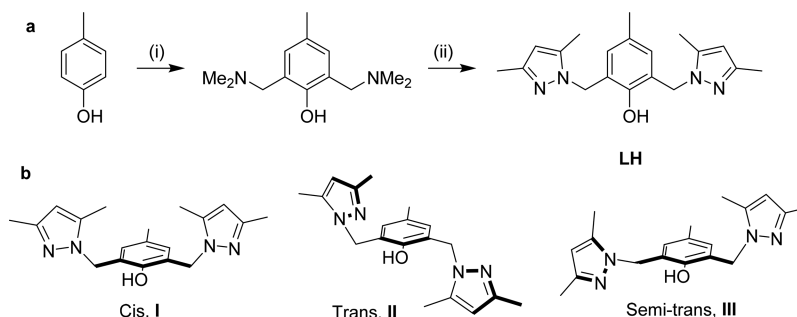
INTRODUCTION

One of the commercially important reactions is the polymerization of norbornene, carried out by three different methods: ring opening metathesis polymerization (ROMP), cationic or radical polymerization, and vinyl-polymerization.¹ As ROMP attracted attention, the vinyl polymerization of norbornene has also received a great deal of attention owing to its attractive physical properties such as mechanical, heat resistivity, transparency properties, high glass transition temperature, low dielectric constant, and good solubility in organic solvents. In addition, the vinyl norbornene polymer is used in making cover layers for liquid-crystals displays and has a cost advantage over related materials. Several metal complexes such as Ti ,² Zr ,³ Cr ,⁴ Co ,⁵ Ni ,⁶ Pd ,⁷ and Cu ⁸ have been reported for the vinyl polymerization of norbornene. Most of these complexes became highly active catalysts upon activation by MAO, MMAO, boranes, and AgSbF_6 salts. Among these, Ni complexes have been shown to be impressively highly active catalysts with activities up to 10^8 g PNB $\text{mol}^{-1} \text{h}^{-1}$.¹⁰ Besides, palladium complexes are also known for their very high activities.⁷ Wang and co-workers have reported highly active NHC-Pd complexes for addition polymerization in the

presence of MAO and Et_2AlCl cocatalysts.¹¹ Recently, Li and co-workers have reported vinyl polymerization in air and water using palladium complexes with the activity up to 10^9 g PNB $\text{mol}^{-1} \text{h}^{-1}$.¹² Furthermore, the polymerization of norbornene derivatives has been reported without a cocatalyst or activator as well.¹³

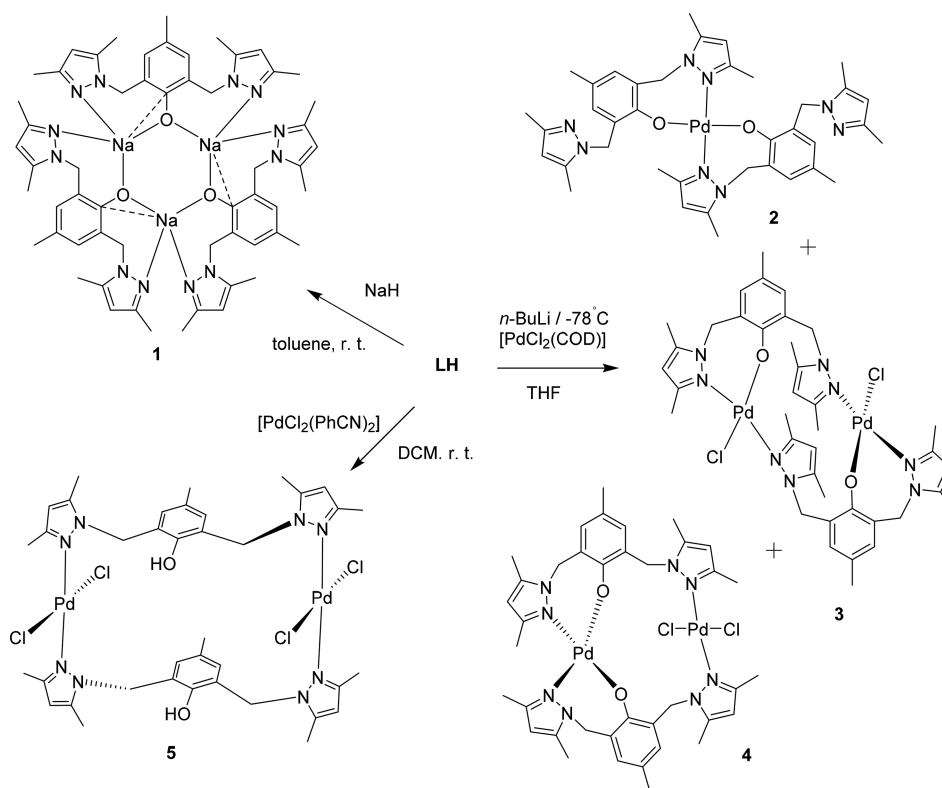
Upon deprotonation with a base, 2,6-bis(3,5-dimethylpyrazolylmethyl)-4-methylphenol **LH** becomes monoanionic tridentate ligand **L** containing a gap of four atoms between the donor atoms. As 2,6-bis[(dimethylamino)methyl]-4-methylphenol does,¹⁴ **L** can also readily bridge as well as chelate metal atoms owing to the presence of two flexible methylene groups on either side of the phenyl ring. The reported synthesis of **LH** or its simple pyrazole analogue involves multiple steps. In addition, its coordination chemistry has not been fully explored except few zinc,¹⁵ copper,¹⁶ and cobalt¹⁷ complexes. Herein, we report the synthesis, X-ray structures, and fluxional properties of the palladium complexes of **LH** which was synthesized by a new method. We also report

Received: March 20, 2018

Scheme 1. (a) Synthesis of 2,6-Bis(3,5-dimethylpyrazolymethyl)-4-methylphenol LH and (b) Possible Conformations of LH^a

^aConditions: (i) HCHO/Me₂NH/H₂O and (ii) 3,5-dimethylpyrazole/xylene/140 °C/12 h.

Scheme 2. Synthesis of the Trisodium, Mononuclear, and Binuclear Pd(II) Complexes of LH



a new trisodium complex of LH and the vinyl polymerization of norbornene using three different palladium complexes in the presence of MMAO or EtAlCl₂ as a cocatalyst.

RESULTS AND DISCUSSION

Synthesis of LH and Its Na and Pd Complexes. As illustrated in Scheme 1a, the synthesis of LH involves two steps from phenol. Without making the quaternary ammonium salt of 2,6-bis[(dimethylamino)methyl]-4-methylphenol, the diamine was directly treated with 3,5-dimethylpyrazole in xylene under reflux conditions followed by chromatographic separation to give *ortho*-bis(3,5-dimethylpyrazolymethyl)phenol ligand LH in good yield (66%). This method of synthesis is similar to that of 2,5-bis(3,5-dimethylpyrazolymethyl)pyrrole¹⁸ and 1,9-bis(3,5-dimethylpyrazolymethyl)dipyrrolylmethane.¹⁹ LH can have three conformations based on the orientation of the pyrazole ring about the phenyl ring plane, as shown in Scheme 1b. The conformations in which

both the pyrazole rings situated above or below the phenyl ring are termed as *cis* (I), one up and down as *trans* (II), and one up and the other in the middle as *semitrans* (III). Interestingly, two of these are observed in their palladium complex structures (see below).

Sodium aryloxides are well-known to have a diverse range of structures such as squares, hexagonal, ladder, and cubic, fused cubic depending upon the nature of ligand.²⁰ In view of this, LH was treated with NaH and an interesting new trinuclear sodium complex, 1, was isolated as crystals (Scheme 2). It crystallizes in the triclinic space group *P* $\bar{1}$, and the asymmetric unit constitutes the whole molecule of 1 together with 1.5 molecules of toluene as solvent of crystallization. The molecular structure of the sodium salt is given in Figure 1 along with selected bond distances and angles. The 6-membered Na₂O₃ ring structure is formed by three anionic ligands L, each spanning two sodium atoms by the bis-chelation mode, and the ring is an almost perfect planar with alternative oxygen and sodium atoms. Each ligand adopts *trans*

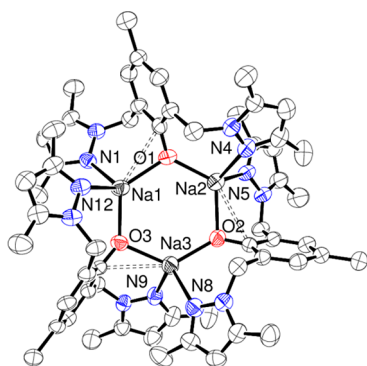


Figure 1. ORTEP diagram of the trinuclear sodium complex **1**. Selected bond distances (Å) and angles (deg). All hydrogens are omitted for clarity. O1–Na2 2.185(3), O1–Na1 2.244(3), O2–Na3 2.181(3), O2–Na2 2.263(3), O3–Na1 2.181(3), O3–Na3 2.252(3), C13–O1 1.313(5), C32–O2 1.314(4), C51–O3 1.295(4), N1–Na1 2.380(3), N12–Na1 2.396(4), N4–Na2 2.406(4), N5–Na2 2.386(4), N8–Na3 2.399(4), N9–Na3 2.382(4), O3–Na1–O1 123.48(12), O3–Na1–N1 113.47(12), O3–Na1–N12 94.12(12), O1–Na1–N1 98.35(12), O1–Na1–N12 125.45(13), N1–Na1–N12 100.55(12). Na2–O1–Na1 120.14(13), Na3–O2–Na2 117.15(12), Na1–O3–Na3 113.65(13), O3–Na1–O1 123.48(12), O1–Na2–O2 119.27(12), O2–Na3–O3 126.17(12).

conformation **II** (Scheme 1b) and bridges two sodium atoms with the bridged bonded phenoxy oxygen atom. This orientation of **L** renders the Na_2O_3 ring with a three-bladed wind-turbine-like structure and screw-type chirality. Both enantiomers are present in the crystal lattice. This is similar to the Li_3O_3 ring reported by van Koten and co-workers.²¹

The ring Na–O–Na and O–Na–O angles are in the ranges of 113.6–120.1° and 119.2–126.1°, respectively. The ring contains an alternatively located shorter (2.181–2.185 Å) and longer (2.244–2.263 Å) Na–O distances, as Kekulé’s benzene structure exhibits. The $\text{C}_{\text{ipso}}\text{–O}$ distances (1.295–1.314 Å) are shorter than that (1.372(4) Å) found in the free ligand structure.²² These bond lengths and angles indicate that the phenoxy oxygen atoms undergone the hybridization change from sp^3 to sp^2 and the oxygen π -electrons are delocalized in the Na_3O_3 ring. The average Na–O distance is 2.217(3) Å, which is slightly shorter than the distances, 2.2263(13),^{20c} 2.29,^{20d} and 2.328(2) Å,^{20e} found in the analogous six-membered sodium structures. In addition, there are three weak bonding interactions of the type $\text{Na}\cdots\text{C}_{\text{ipso}}$ (2.840, 2.888, and 2.909 Å) in the ring, which are slightly longer than those reported for the analogous sodium structure.^{20c} The geometry around each sodium atom is a distorted tetrahedral formed by two pyrazole nitrogens and two bridging oxygens with N–Na–N angles (100.55(12)–103.76(14)°) being smaller than the O–Na–O angles (119.28(12)–126.18(12)°). Interestingly, the geometry around each ring oxygen atom is trigonal planar and the sum of the angles around each oxygen atom (358.1, 355.1, and 357.3°) is close to 360°, indicating sp^2 hybridization. The three-bladed turbine-like orientation of three ligands about the Na_3O_3 ring is not rigid in solution, as shown by its ^1H NMR spectrum which featured a broad singlet at δ 5.21 ppm for all the methylene protons, indicating the dynamic behavior of molecule in solution.

As shown in Scheme 2, the reaction between deprotonated ligand **L** and $[\text{PdCl}_2(\text{COD})]$ in THF gave three Pd(II) complexes **2–4**, whereas the reaction of neutral ligand **LH** with

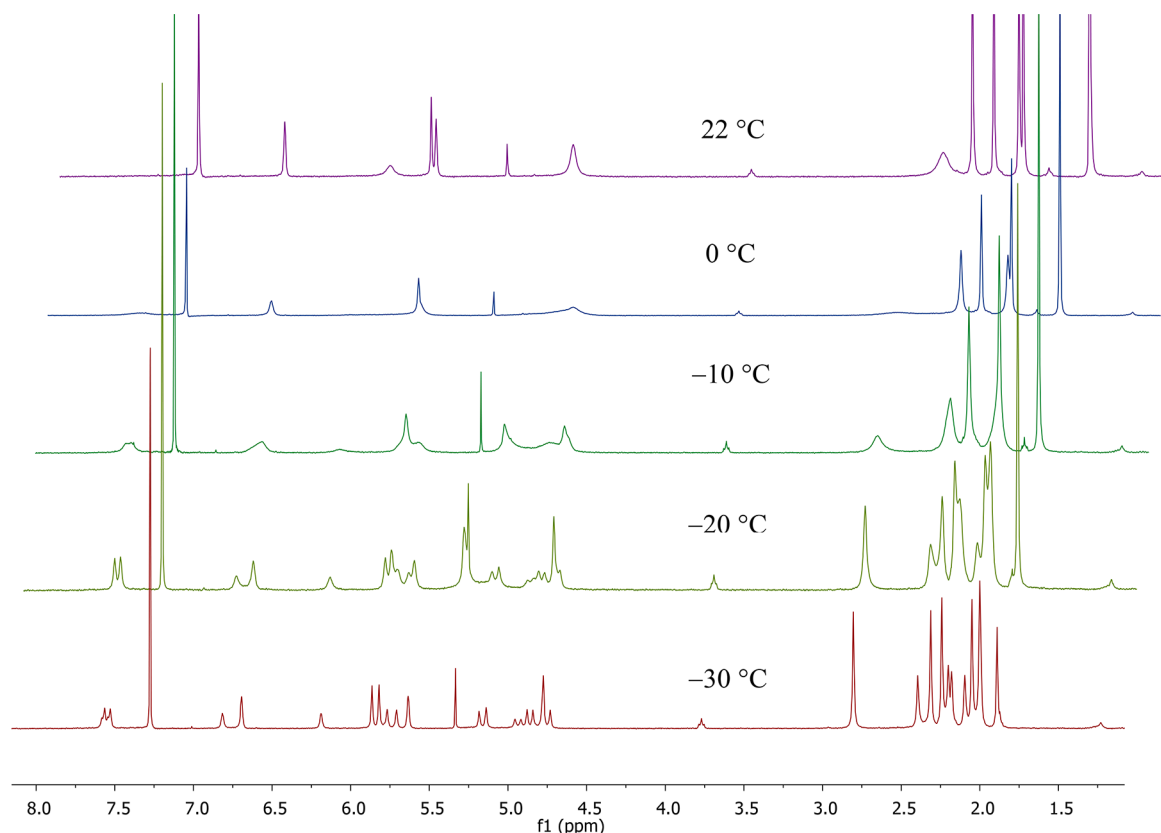


Figure 2. Variable-temperature (VT) ^1H NMR spectra (400 MHz) of **2** in CDCl_3 .

[PdCl₂(PhCN)₂] afforded yet another binuclear Pd(II) complex **5** in 46% yield. Crystals of **2–4** were formed together from the reaction mixture upon crystallization and were separated by handpicking as they have different crystal morphology and colors with crystalline yields of 9, 18, and 17%, respectively. In addition, complex **2** was also obtained from the reaction among **LH**, NaH, and [PdCl₂(COD)] in THF in 47% yield. Furthermore, the ¹H NMR spectrum of the residue obtained from the reaction between complex **5** and 2 equiv of NaH showed the formation of complex **3**, a major product. All complexes are characterized by both spectroscopic and single crystal X-ray diffraction methods. The unforeseen chelation and bridging mode of **LH** ($\mu_2\text{-}\kappa^2\text{NO}:\kappa^1\text{N}$) in **3** and **4** are shown by their ¹H NMR spectra recorded in CDCl₃. Two AB quartets are observed for the two different diastereotopic methylene groups with different coupling constants (for example, $J(\text{H}_\text{A}\text{H}_\text{B}) = 14.2$ and 17.4 Hz for complex **3**). Furthermore, the unsymmetrical coordination mode of **LH** is also indicated by the number of peaks appeared for the pyrazole methyl, CH and phenyl CH protons. In addition, their ¹³C NMR spectra showed 19 peaks for the 19 different carbon atoms in the structure.

Conversely, the ¹H NMR spectra of complex **2** and **5** in CDCl₃ displayed broad resonances for their methylene protons, suggesting fluxional behaviors in solution. Complex **2** possesses two different pyrazole arms, coordinated and spectator, but its room-temperature spectrum featured only one broad singlet for the diastereotopic methylene protons as well as for the phenyl protons. Hence, it was studied by VT NMR method. As the temperature is decreased, a well resolved complicated spectrum featuring AB quartets for the diastereotopic methylene protons was obtained at -30 °C (Figure 2). From the number (three) and integrated intensity of the signals in the aromatic region, at least two complexes are in a dynamic process. As the spectrum appears complicated, the dynamic process could be the interconversion between the trans (observed in the solid state) and cis structures through the $\kappa^1\text{O}$ coordination mode of **LH** or dissociation-association processes, as shown in Figure 3. Its activation energy barrier (ΔG^\ddagger) calculated based on the methylene proton resonances at δ 5.15 and 4.74 ppm at -30 °C which merge into a broad peak at the coalescence temperature (T_c) 0 °C (273.15 K) is 53.3 kJ/mol with $\Delta\nu = 163.2$ Hz and $k_c = 362.5$ s⁻¹.

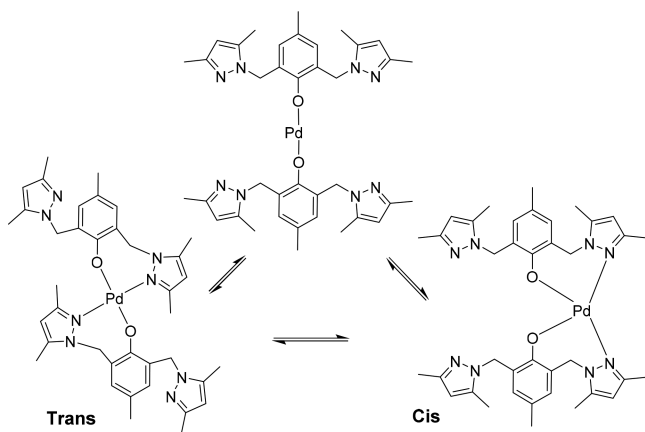


Figure 3. Proposed dynamic process of **2** in CDCl₃ solution: interconversion between the trans and cis complexes through the two coordinate Pd(II) complex, as studied by VT ¹H NMR method.

The room-temperature ¹H NMR spectrum of **5** in CD₂Cl₂ featured broad resonances at δ 5.53, 6.00, and 6.86 ppm for the diastereotopic methylene, pyrazole, and phenyl CH protons, respectively. This indicates a dynamic process occurring in solution and prompted us to investigate it by VT ¹H NMR method. As shown in Figure 4, the ¹H NMR spectra were recorded for every 10 °C decrease in temperature up to -70 °C. As the temperature is decreased, the above-mentioned signals broadened, and four doublets for the methylene protons and two singlets each for the pyrazole and phenyl ring protons then appeared at -70 °C. The coalescence temperature is -50 °C, after which two signals appeared for the phenyl ring CH protons. This dynamic behavior is due to the interconversion between the two enantiomers, as shown in Figure 5, one of which is present in the asymmetric unit of the crystal lattice. The X-ray structure of this complex showed that, for a given ligand, the three ring planes, that is, two pyrazole and one phenyl, are perpendicular to each other and molecule possesses a C₂ axis. In the interconversion process, one enantiomer is changed to another by ring-flipping process in which the two pyrazole rings swap their planes about the phenyl ring plane, that is, the pyrazole ring lying above the phenyl ring changes to the pyrazole ring lying middle to the phenyl plane and vice versa. At room temperature, the rate of pyrazole ring plane swapping is faster so that the diastereotopic methylene H_AH_B are changed to H_CH_D protons and vice versa, and they appear as a single broad resonance. At low temperature (-70 °C), the plane swapping is arrested or slowed down, and they give a well-resolved spectrum with the average coupling constant $J(\text{H}_\text{A}\text{H}_\text{B}) = 19$ Hz for the methylene protons. In addition, this arrested pyrazole ring orientation renders two different chemical environments for each phenyl and pyrazole CH protons and four different environments for the pyrazole methyl groups; hence, they all appear as singlets at the -70 °C spectrum. Its activation energy barrier (ΔG^\ddagger) was calculated based on the phenyl proton resonances at δ 6.88 and 5.58 ppm at -70 °C which merge into a broad peak at the coalescence temperature (T_c) -50 °C (223.15 K) is 24.7 kJ/mol with $\Delta\nu = 520$ Hz and $k_c = 1154.9$ s⁻¹.²³

The X-ray structure of complex **2** is given in Figure 6 along with selected bond lengths and angles. It crystallizes in the monoclinic centrosymmetric space group $P2_1/c$, and the asymmetric unit constitutes a half molecule. The symmetry generated molecule revealed that it consists of one palladium atom coordinated by two ligands via its deprotonated phenolic oxygen and pyrazole nitrogen atoms, forming two seven-membered puckered chelate rings. The other pyrazole arm of each ligand remains as a spectator. As a result, the molecule is fluxional in solution. The geometry around the palladium atom is a distorted square planar in which the phenoxy oxygens or pyrazole nitrogens are trans bonded with the O1–Pd1–N1 and O1ⁱ–Pd1–O1 angles of 92.74(11) and 180.0°, respectively. The N1–Pd1 bond distance of 2.009(3) Å falls within the range of distances reported for complexes containing Pd–N_{pyrazole} bonds^{24,19} and is shorter than the Pd–N_{Me2} distance (2.082(5) Å) found in [Pd(OC₆H₂(CH₂NMe₂)₂-2,6-Me-4)₂].²⁵ The O1–Pd1 bond distance of 2.0004(19) Å is close to those found in palladium complexes containing Pd–O bonds [1.974(11) and 1.989(10) Å,²⁶ 1.994(4) and 1.987(4) Å],²⁷ but it is slightly shorter than 2.021(4) Å found in [Pd(OC₆H₂(CH₂NMe₂)₂-2,6-Me-4)₂].²⁵

Complex **3** crystallizes in the noncentrosymmetric orthorhombic space group Aba_2 and the asymmetric unit contains a

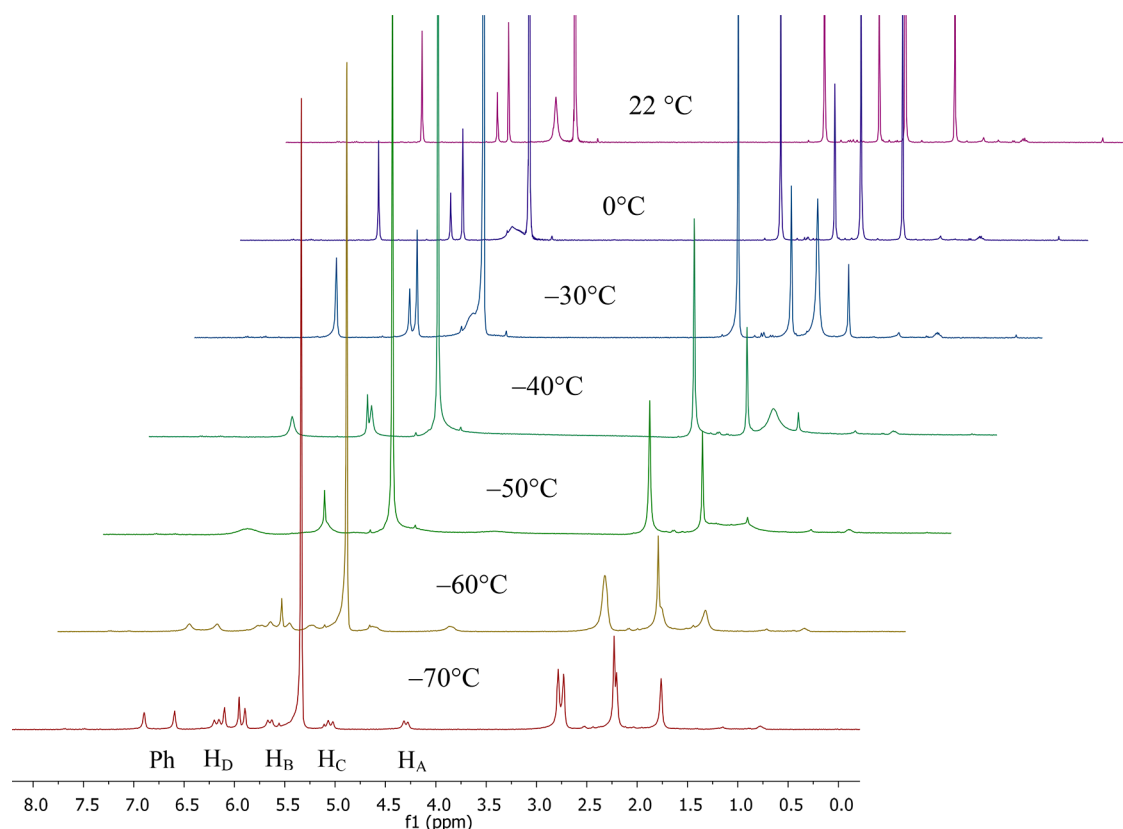


Figure 4. VT ^1H NMR spectra (400 MHz) of **5** in CD_2Cl_2 .

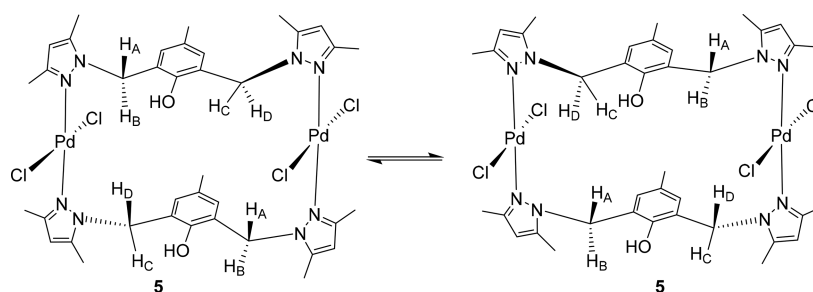


Figure 5. Dynamic behavior of complex **5** in CD_2Cl_2 studied by VT ^1H NMR method.

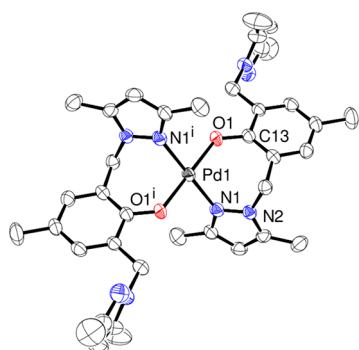


Figure 6. X-ray structure of complex **2** with 50% probability ellipsoids. All hydrogen atoms are omitted for clarity. Selected bond distances (Å) and angles (deg): N1–Pd1 2.009(3), O1–Pd1 2.0004(19), C13–O1 1.337(4), N1–N2 1.366(4), O1–Pd1–N1 92.74(11), O1–Pd1–N1 i 87.26(11), O1 i –Pd1–O1 180.0, N1–Pd1–N1 i 180.0. Symmetry transformations used to generate equivalent atoms: $^i = -x + 2, -y, -z + 1$.

half molecule of **3** and a half molecule of water. The full molecule was generated by C_2 rotation and is given in Figure 7 along with selected bond distances and angles. The X-ray structure revealed two Pd–Cl units bridged by two phenolate ligands **L**. Each ligand renders one seven-membered chelate ring formed by the coordination of one of the pyrazole nitrogens and the phenolate oxygen atom, while it bridges the other palladium atom via the other pyrazole nitrogen atom. Thus, each ligand displays both bridging and chelating modes, represented as $\mu_2\text{-}\kappa^2\text{NO}:\kappa^1\text{N}$. As a result, there are two seven- and one 14-membered palladacycles in the structure and the molecule exhibits a tub shape containing one water molecule hydrogen bonded to the phenolate oxygen atoms. To maintain a square planar geometry around each palladium atom, both pyrazole arms are twisted and ligand assumes the trans conformation **II**. The angle between the mean planes of the pyrazole rings or the phenyl rings is 74.4 or 87.4° , respectively. The twist angle between the palladium square plane and the phenyl ring plane is 46.9° . In addition, the angle between the two palladium square planes is 72.8° . This configuration is

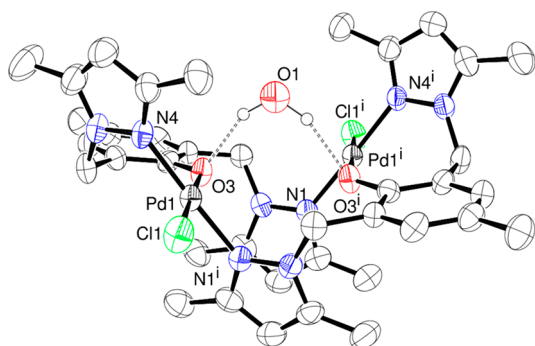


Figure 7. X-ray structure of complex **3** with 50% probability ellipsoids. Most hydrogen atoms are omitted for clarity. Selected bond distances (Å) and angles (deg): N4–Pd1 2.009(4), N1–Pd1 2.020(4), O3–Pd1 2.018(3), Cl1–Pd1 2.2846(12), N4–Pd1–O3 90.19(18), N4–Pd1–N1 177.89(16), O3–Pd1–N1 88.68(17), N4–Pd1–Cl1 92.24(13), N1–Pd1–Cl1 88.92(12). Symmetry transformations used to generate equivalent atoms: $i = -x + 2, -y, z$.

rigid with the help of water molecule hydrogen bondings in the cavity, and as a result, its ^1H NMR spectrum showed well resolved peaks. The angle between the trans pyrazole nitrogen atoms and the Cl–Pd–O angle are almost the same, 177.9(1) and 177.5(1) $^\circ$, respectively. The nonbonding Pd⋯Pd distance is 5.44 Å. The structure contains two slightly different Pd–N_{pyrazole} distances: 2.009(4) and 2.020(4) Å; nevertheless, these are very close to the Pd–N distances found in complex **2** and **4** and are in the range reported for other complexes.²⁴ The Pd–O bond distance of 2.018(3) Å is close to the Pd–O bond in [Pd(OC₆H₄(CH₂NMe₂)₂-2,6-Me-4)₂]²⁵ but is slightly longer than that found in other palladium complexes.^{26,27}

The X-ray structure of complex **4** is given in Figure 8 with selected bond distances and angles. It crystallizes in the centrosymmetric space group $P2_1/c$, and the asymmetric unit consists of one full molecule and two dichloromethanes. Although this binuclear palladium complex contains the same metal to ligand ratio, bonding mode of L, and number of palladacycles as those in complex **3**, it is structurally different

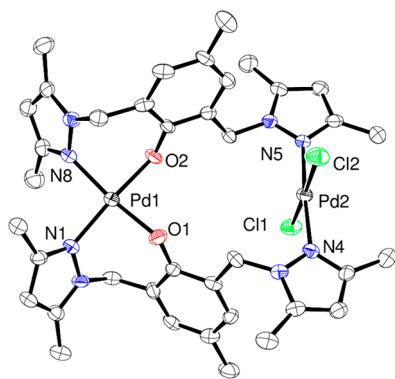


Figure 8. X-ray structure of complex **4** with 50% probability ellipsoids. All hydrogen atoms and CH₂Cl₂ are omitted for clarity. Selected bond distances (Å) and angles (deg): N1–Pd1 2.012(5), N8–Pd1 2.007(5), O1–Pd1 1.981(4), O2–Pd1 2.006(4), N4–Pd2 2.018(5), Cl1–Pd2 2.2856(18), Cl2–Pd2 2.2964(18), N5–Pd2 1.999(5), N8–Pd1–N1 95.5(2), O1–Pd1–O2 88.08(18), O1–Pd1–N1 90.08(19), O2–Pd1–N8 87.42(19), O1–Pd1–N8 170.6(2), O2–Pd1–N1 171.9(2), N5–Pd2–N4 176.1(2), Cl1–Pd2–Cl2 177.14(6), N5–Pd2–Cl1 90.27(16), N4–Pd2–Cl1 89.98(15), N5–Pd2–Cl2 87.09(16), N4–Pd2–Cl2 92.72(15).

because of the different conformation adopted by L. Interestingly, unlike the structure of **3**, only one of the pyrazole rings is above or below the phenyl ring plane, and the other remains middle to the phenyl ring, that is, each ligand adopted the semitrans conformation **III**. As a result, the mean planes of phenyl and two pyrazole rings are approximately perpendicular to each other. The coordination environment around one palladium atom exhibits two seven-membered chelate rings, whereas the other metal contains two pyrazole nitrogens and two chlorine atoms in a trans fashion. Hence, complexes **3** and **4** are structural isomers in which the metal centers differ by the coordinated ligands. The two distorted palladium square planes are almost perpendicular to each other with the angle of 83.3 $^\circ$. At the bischelated palladium atom, the N8–Pd1–N1 (pyrazole nitrogen) angle of 95.5(2) $^\circ$ is larger than the O1–Pd1–O2 (phenoxy oxygen) angle (88.08(18) $^\circ$), probably because of steric crowding caused by 3,5-dimethylpyrazole rings. Conversely, the N–Pd–N angle at the other palladium atom is almost linear, 176.1 $^\circ$. The Pd–N_{pyrazole} bond distances are similar to those in complex **3** or **2**, and the Pd–O bond distances are slightly shorter than the distance (2.018(3) Å) found in **3**.

Complex **5** crystallizes in the triclinic space group $P\bar{1}$, and the asymmetric unit consists of two molecules of **5** held together by hydrogen bondings of the type OH⋯Cl–Pd along with one dichloromethane and four water molecules. The hydrogen bonded dimeric structure is shown in Figure 9. Each

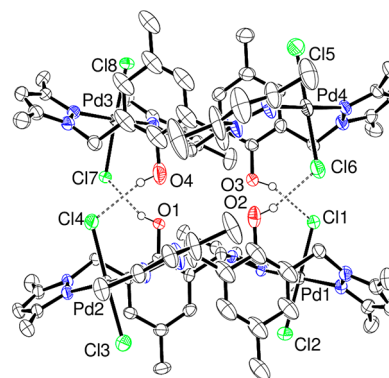


Figure 9. X-ray structure of complex **5** with 50% probability ellipsoids. Most hydrogen atoms, CH₂Cl₂, and water are omitted for clarity. Selected bond distances (Å) and angles (deg): N1–Pd1 1.999(5), N8–Pd1 2.020(5), N4–Pd2 2.024(4), N5–Pd2 1.996(5), Cl1–Pd1 2.3223(16), Cl2–Pd1 2.2867(16), Cl3–Pd2 2.2946(17), Cl4–Pd2 2.3143(16), Cl2–Pd1–Cl1 177.12(7), N1–Pd1–N8 178.0(2), N1–Pd1–Cl2 90.14(14), N8–Pd1–Cl2 90.40(15), N1–Pd1–Cl1 87.68(14), N8–Pd1–Cl1 91.71(15), N5–Pd2–N4 174.5(2), N5–Pd2–Cl3 90.69(17), N4–Pd2–Cl3 90.66(14), N5–Pd2–Cl4 87.38(17), N4–Pd2–Cl4 91.29(14), Cl3–Pd2–Cl4 178.06(6). Hydrogen bonding parameters: O1⋯Cl7 3.178(4), H1⋯Cl7 2.40, O1–H1⋯Cl7 160.0; O2⋯Cl6 3.178(5), H2⋯Cl6 2.38, O2–H2⋯Cl6 164.6; O3⋯Cl1 3.145(5), H3A⋯Cl1 2.40, O3–H3A⋯Cl1 152.0; O4⋯Cl4 3.212(6), H4⋯Cl4 2.41, O4–H4⋯Cl4 166.5.

molecule consists of two “PdCl₂” moieties bridged by two neutral LH ligands via their pyrazole nitrogens, forming the 20-membered palladacycle in which the two palladium square planes are almost parallel to each other, as do the phenyl ring planes. The aryl OH groups are pointed to the same direction and involved in hydrogen bonding interactions to the adjacent molecule. Each ligand adopts the “semitrans” conformation

Table 1. Catalysis of Norbornene Polymerization by Complexes 3–5 with MMAO-12 as a Cocatalyst^a

entry	catalyst (μmol)	MMAO (mmol)	solvent (mL)	[NB]/[Cat]	[Al]/[Cat]	PNB (g) ^b	yield (%)	activity ^c
1	5 (1)	1	toluene (9)	21240	1000	1.43	71	8.61×10^7
2	5 (1)	1	toluene (19)	21240	1000	1.35	67	8.12×10^7
3	5 (2)	1	toluene (9)	10620	500	1.638	82	4.91×10^7
4	5 (2)	1	toluene (19)	10620	500	1.33	66	4.00×10^7
5	5 (3)	1	toluene (9)	7080	333	1.32	66	2.64×10^7
6	5 (1)	0.1	toluene (9.9)	21240	100	0.16	8	0.96×10^6
7	5 (1)	2	toluene (8)	21240	2000	1.87	93	1.12×10^8
8	5 (1)	3	toluene (7)	21240	3000	1.911	95	1.15×10^8
9	5 (1)	1	CH ₂ Cl ₂ (9)	21240	1000	1.995	~100	1.20×10^8
10	5 (1)	0.5	CH ₂ Cl ₂ (9.5)	21240	500	0.410	20	2.46×10^7
11	3 (1.1)	1	toluene (9)	19309	909	0.610	30	3.09×10^7
12	3 (1.1)	2	toluene (8)	19309	1818	1.47	73	8.20×10^7
13	3 (1.1)	1	CH ₂ Cl ₂ (9)	19309	909	1.32	66	7.53×10^7
14	3 (1.1)	2	CH ₂ Cl ₂ (8)	19309	1818	1.90	95	1.06×10^8
15	4 (1.1)	1	CH ₂ Cl ₂ (9)	19309	909	0.986	49	5.50×10^7
16	4 (1.1)	2	CH ₂ Cl ₂ (8)	19309	1818	1.932	96	1.07×10^8
17	[PdCl ₂ (COD)] (10)	1	toluene (9)	2124	100	0.173	8.6	5.20×10^5
18	[PdCl ₂ (COD)] (1)	1	toluene (9)	21240	1000	0.060	3	3.42×10^6
19	[PdCl ₂ (PhCN) ₂] (1.56)	1.56	toluene (8.5)	13579	1000	1.701	85	6.52×10^7
20	PdCl ₂ (1)	1	toluene (9)	21240	1000	0.500	25	1.50×10^7

^aIn all cases, 2.0 g of norbornene was used, and the reactions were carried out at room temperature. ^bQuantity of polymer after 1 min, except entries 17 and 20 for which the reaction time is 2 min, and for entry 6, it is 10 min. ^cGiven in g PNB mol⁻¹ h⁻¹. The molecular weight of complex 3 or 4 is 930.58 g, and that of 5 is 1003.49 g without any solvent crystallization as supported by their CHN analyses.

(III) in which one of the pyrazole rings lies above the phenyl ring and the molecule possesses a C₂ axis, rendering both palladium atoms to be in one environment. Both molecules in the dimer represent one chiral enantiomer and the opposite enantiomer is present in the crystal lattice. The average distance between the two palladium atoms is 8.71 Å. The geometry around each palladium atom is a distorted square plane containing two trans pyrazole nitrogen and chloride atoms with the average N–Pd–N and Cl–Pd–Cl angles of 176.1 and 177.5°, respectively. The Pd–N distances range from 1.996(5) to 2.024(4) Å and are similar to those found in previous complexes 3 and 4.

Vinyl Polymerization of Norbornene. The vinyl polymerization of norbornene was carried out with new complexes 3–5, and the conditions and activities are summarized in Table 1. When the reaction was carried out with 1 μmol of complex 5 and 1000 molar excess of MMAO in toluene, the yield of polynorbornene is 71% in 1 min, and the activity is 8.61×10^7 g PNB mol⁻¹ h⁻¹. The yield of PNB is increased to 82% with the increased catalyst loading of 2 μmol ([Al]/[Cat] = 500) and then decreased with further increase in the catalyst loading of 3 μmol ([Al]/[Cat] = 333). A poor yield and activity was obtained with the aluminum to catalyst ratio of 100 (entry 6). In addition, we also found that the activity is slightly decreased under the relatively dilute conditions (entries 2 and 4). Conversely, when the [Al]/[Cat] ratio is increased to 2000 or 3000, the yield of the polymer is significantly increased to greater than 90% yields with the activity shoot up of 1.15×10^8 g PNB mol⁻¹ h⁻¹ in toluene (entry 7 and 8). It suggests that MMAO plays an important role in stabilizing the active metal center to give a greater yield and activity. This encouraged us to carry out the polymerization in a different solvent to observe the activity difference. Thus, when the reaction was carried out in dichloromethane with the 1000 molar excess of aluminum, an almost quantitative yield of PNB was obtained with activity of 1.20×10^8 g PNB mol⁻¹ h⁻¹ (entry 9). However, the yield

and activity is decreased as the aluminum ratio is decreased to 500. Hence, entry 9 represents the optimized conditions for the greater activity; it is one of the highly active palladium catalysts reported to date. Furthermore, it suggests CH₂Cl₂ is a better solvent than toluene. The same polymerization reactions were also carried out with complex 3 and 4. The yield and activity is increased, as the aluminum ratio is increased from 1000 to 2000 in dichloromethane or toluene (1.06×10^8 g PNB mol⁻¹ h⁻¹, entry 14). This activity is comparable to that of complex 5 in dichloromethane with the aluminum to catalyst ratio of 1000, suggesting that complex 5 is a better catalyst as compared to complex 3 or 4. Furthermore, polymerizations were also carried out with precursors: PdCl₂, [PdCl₂(COD)], and [PdCl₂(PhCN)₂]. Although all catalyze the vinyl polymerization of norbornene in combination with MMAO in toluene at room temperature, their activities are different, as given in Table 1 (entries 17–20). While PdCl₂ and [PdCl₂(COD)] activities are lower, [PdCl₂(PhCN)₂] activity is almost equal to those given by complex 3, 4, or 5, suggesting that similar type of active metal center is involved in the polymerization reactions catalyzed by complex 3, 4, or 5. Furthermore, catalysis reactions with 1000 molar excess of MMAO in toluene at 50 or 100 °C did not give polynorbornene precipitate, and the reaction mixture turned to a black turbid suspension, indicating decomposition of the catalyst at higher temperatures.

Polynorbornenes obtained from all these reactions are only sparingly soluble in chlorobenzene. The ¹H NMR spectrum of polynorbornene in chlorobenzene-*d*₃ showed two major broad signals at $\delta = 1.17$ and 2.30 ppm and no peak in the region around 5.5 ppm. In addition, no stretching frequency was observed in the range 1620–1680 cm⁻¹ in the IR spectrum. Hence, the polymers are formed by the vinyl addition of norbornene, not ring opening. The TGA showed polymers are stable up to 450 °C, a characteristic property of polynorbornene as reported in several cases. The X-ray diffraction

Table 2. Norbornene Polymerizations with EtAlCl₂ as a Cocatalyst

entry	catalyst (μmol)	EtAlCl ₂ (mmol)	solvent (mL)	time (min)	[NB]/[Cat]	[Al]/[Cat]	PNB (g)	yield (%)	activity ^a
1	5 (1)	1	toluene (9.5)	1	21240	1000	0.907	45	5.46×10^7
1	5 (1)	1	toluene (9.5)	2	21240	1000	1.716	86	5.16×10^7
2	5 (1)	1	toluene (9.5)	3	21240	1000	1.87	93	3.75×10^7
3	5 (1)	2	toluene (9)	1	21240	2000	1.31	65	7.88×10^7
4	5 (1)	2	toluene (9)	3	21240	2000	1.89	94	3.79×10^7
5	3 (1.1)	1	toluene (9.5)	1	19309	909	1.998	100	1.09×10^8
6	4 (1.1)	1	toluene (9.5)	1	19309	909	2.233 ^b	111	1.13×10^8

^aGiven in g PNB mol⁻¹ h⁻¹. ^bGreater than 2 g probably because of water as shown by IR spectrum, which could not be removed at 80 °C under vacuum.

pattern showed noncrystalline nature of the polymer and is similar to the literature reports (see Supporting Information).^{7c,f} However, it is insoluble in THF, dichloromethane, and CHCl₃, which precluded us from characterization by GPC method.

The norbornene polymerization catalysis was also carried out with EtAlCl₂ as a cocatalyst. We applied the best conditions of polymerization obtained with MMAO to polymerize norbornene in combination with EtAlCl₂, and complex 3, 4, or 5, and the results are summarized in Table 2. Complex 5 catalyzes the polymerization in the presence of 1000 or 2000 molar excess of EtAlCl₂, and their yields increase as time increases from 1 to 3 min (entry 1–4). The 1000 molar excess reaction in 3 min gave the maximum yield. In contrast to this, the catalyzes reactions using either complex 3 or 4 afforded quantitative yields of polymers in the presence of 909 molar excess of EtAlCl₂ in toluene in 1 min, and their activities are in the range of 10⁸ g PNB mol⁻¹ h⁻¹ (entry 5 and 6), showing both complexes as highly active catalysts. In addition, polymerization reactions using 3, 4, or 5 in the presence of 400 or 1000 molar excess of AlMe₃ gave no precipitate.

In contrast to the powdery nature of polymers obtained with MMAO, polymers obtained with EtAlCl₂, in most cases are a viscous oily film or gel-type precipitate which turned to one piece of colorless almost transparent chunk upon hydrolysis and air drying. In some cases, it appears similar to the MMAO polymer. Again, the dried polymer is insoluble in solvents such as CH₂Cl₂, CHCl₃, toluene, THF, acetone, CH₃CN, and diethyl ether. The IR spectrum of this polymer showed a broad band at 3422 cm⁻¹, indicating the presence of OH groups. The TGA of this polymer is different from that of MMAO polymers in terms of mass changes. Decomposition occurs from 100 °C onward and then appears to be similar to the mass change profile of MMAO polymers. The polymer was again not characterized by GPC method as it remains completely insoluble in solvents mentioned above.

CONCLUSIONS

In conclusion, we have developed a new synthetic method for the bis(pyrazolylmethyl)phenol ligand LH. In addition to the mononuclear palladium complex containing the spectator ligand, the unforeseen coordination mode of LH, μ_2 - $\kappa^2\text{NO}:\kappa^1\text{N}$ in 3 and 4, was also observed, proving its flexibility in choosing the bonding modes: mono- and bischelation and bridging. As a result, benzene-like enantiomers and structural isomers containing trans and semitrans conformations of LH were structurally characterized. Interestingly, while complexes 3 and 4 are stereochemically rigid, complex 5 with its simple bridging mode of LH and complex 2 are fluxional and their

interconversions are studied by VT NMR methods, providing insights into the structures in solutions. Importantly, all the three binuclear palladium complexes 3–5 are precatalysts for the vinyl polymerization of norbornene in combination with MMAO and EtAlCl₂ at room temperature. Almost all the monomers are converted into polymers within a short period of time 1 min, representing them as highly active catalysts. Near quantitative yields and very high activities under mild conditions such as low catalyst loading, relatively low [Al]/[Pd] ratio, and room temperature are favorable attributes of the polymerization reactions reported here. Homopolymerization of norbornene and copolymerization with other olefins using Ni(II) and Pd(II) complexes containing other ligand systems are under progress.

EXPERIMENTAL SECTION

General Procedure. All reactions were carried out under a nitrogen atmosphere using standard Schlenk line techniques or nitrogen-filled glovebox. Petroleum ether (bp 40–60 °C) and other solvents were distilled under N₂ atmosphere according to the standard procedures. Norbornene, modified methylaluminoxane (MMAO-12, 7 wt % in toluene), EtAlCl₂ (25 wt % in toluene), and Me₃Al (2 M in toluene) were purchased from Aldrich and used as received except norbornene which was distilled over sodium under vacuum. Other chemicals were obtained from commercial sources and used as received. [PdCl₂(COD)]²⁸ and [PdCl₂(PhCN)₂]²⁹ were synthesized according to the reported procedures. ¹H (400 MHz) and ¹³C (102.6 MHz) NMR spectra were recorded at room temperature. For ¹H NMR spectra, chemical shifts are referenced with respect to the chemical shift of the residual protons present in the deuterated solvents, and for ¹³C NMR spectra, the CDCl₃ chemical shift was used as a reference. Chemical shifts are in parts per million, and coupling constants are in Hz. FTIR and ATR spectra were recorded using PerkinElmer Spectrum Rx. High-resolution mass spectra (ESI) were recorded using the Xevo G2 Tof mass spectrometer (Waters). Elemental analyses were carried out using a PerkinElmer 2400 CHN analyzer. Thermogravimetric analysis (TGA) was recorded on a TG 209 F3 Tarsus (Netzsch) in which polymer samples were heated from room temperature to 800 °C at a rate of 10.0 K per minute under a nitrogen atmosphere.

Synthesis of 2,6-Bis(3,5-dimethylpyrazolylmethyl)-4-methylphenol LH. To a solution of 2,6-bis[(dimethylamino)methyl]-4-methylphenol (5.00 g, 22.5 mmol) in xylene (50 mL) was added 3,5-dimethylpyrazole (4.54 g, 47.2 mmol) and stirred for 12 h under reflux conditions. The solvent was removed under vacuum, and the resulting residue was loaded onto a silica gel column and eluted with EtOAc/petroleum ether (v/v = 1:5). The solvents were removed from the first fraction to give 4.80 g of LH (14.8 mmol, yield: 66%). ¹H NMR (CDCl₃, 400 MHz): δ 10.88 (s, 1H, phenyl–OH), 6.66 (s, 2H, phenyl–CH), 5.79 (s, 2H, pyrazole–CH), 5.13 (s, 4H, CH₂), 2.24 (s, 6H, pyrazole–CH₃), 2.22 (s, 6H, pyrazole–CH₃), 2.15 (s, 3H, phenyl–CH₃).

Synthesis of [NaOC₆H₂(CH₂Pz^{Me2})₂-2,6-Me-4]₃ 1. NaH (0.025 g, 60% in mineral oil, 0.625 mmol) was taken in a 250 mL Schlenk

flask, washed with petroleum ether (3 × 5 mL), and then dried under vacuum. To the resulting NaH powder was added toluene (30 mL) followed by LH (0.150 g, 0.462 mmol) at room temperature. The solution was stirred for 12 h and layered with petroleum ether (50 mL). Colorless crystals of complex 1 were formed over a period of 3 days at room temperature. Crystals were separated and dried under vacuum (0.070 g, 0.059 mmol). Yield: 38%. ¹H NMR (C₆D₆, 400 MHz): δ 6.95 (s, 6H, phenyl-CH), 5.52 (s, 6H, pyrazole-CH), 5.21 (br s, 12H, CH₂), 2.25 (s, 9H, phenyl-CH₃), 1.96 (s, 18H, pyrazole-CH₃), 1.68 (s, 18H, pyrazole-CH₃). ¹³C NMR (C₆D₆, 102.6 MHz): δ 147.1, 138.8, 131.5, 128.1, 126.0, 104.7, 49.2, 20.7, 12.6, 11.4. FTIR (Nujol, cm⁻¹): 2924 (vs), 2855 (vs) 2729 (w), 1611 (w), 1549 (m), 1354 (m), 1335 (m), 1311 (m), 1255 (m), 1158 (w), 1118 (vw), 1034 (w), 983 (w), 919 (vw), 872 (vw), 825 (w), 806 (w), 785 (w), 768 (m), 722 (m), 629 (vw), 596 (vw), 562 (w), 544 (w), 504 (vw), 475 (w), 460 (w).

Synthesis of [Pd{OC₆H₂(CH₂Pz^{Me2})₂-2,6-Me-4-κN,O₂}]₂ 2, [PdCl{μ-OC₆H₂(CH₂Pz^{Me2})₂-2,6-Me-4-κN,O,N₂}]₂ 3, and [PdCl₂{μ-OC₆H₂(CH₂Pz^{Me2})₂-2,6-Me-4-κN,O,N₂}Pd]₂ 4. To a solution of LH (0.108 g, 0.333 mmol) in THF (30 mL) was added *n*-BuLi (0.22 mL, 0.352 mmol, 1.6 M in hexane) at -114 °C. The solution was allowed to come to room temperature, and then [PdCl₂(COD)] (0.050 g, 0.175 mmol) was added and stirred for 12 h at room temperature. The solvent was removed under vacuum and the resulting reddish brown residue was dissolved in dichloromethane (30 mL), filtered, and then layered with petroleum ether (60 mL). A dark red colored sphere shaped crystals of complex 2, yellow colored prism shaped crystals of complex 3, and yellow colored needle shaped crystals of complex 4 were formed in the same flask over a period of 10 days and separated by hand picking. All crystals were washed with petroleum ether and dried under vacuum: 2 (0.012 g, 0.016 mmol, yield: 9%), 3 (0.015 g, 0.016 mmol, yield: 18%), and 4 (0.014 g, 0.015 mmol, yield: 17%).

[Pd{OC₆H₂(CH₂Pz^{Me2})₂-2,6-Me-4-κN,O₂}]₂ 2. Mp > 200 °C. ¹H NMR: (CDCl₃, 400 MHz): δ 6.71 (s, phenyl-CH), 6.04 (br s, phenyl-CH), 5.78 (s, pyrazole-CH), 5.75 (s, pyrazole-CH), 4.87 (br s, CH₂), 2.51 (br s, phenyl-CH₃), 2.34 (s, pyrazole-CH₃), 2.20 (s, pyrazole-CH₃), 2.04 (s, pyrazole-CH₃), 2.02 (s, pyrazole-CH₃). ¹³C NMR (CDCl₃, 102.6 MHz): δ 161.0, 149.9, 147.2, 140.5, 139.6, 129.3, 128.6, 128.2, 122.8, 118.9, 107.6, 104.8, 51.5, 49.0, 20.5, 13.80, 13.76, 11.7, 10.9. FTIR (KBr, cm⁻¹): 3432 (br), 3124 (vw), 3086 (vw), 2922 (m), 2859 (w), 1613 (m), 1554 (m), 1457 (vs), 1428 (s), 1389 (w), 1341 (w), 1308 (s), 1259 (s), 1162 (m), 1069 (w), 1032 (w), 973 (w), 869 (w), 802 (m), 769 (m), 705 (w), 660 (vw), 616 (vw), 568 (w), 522 (w), 434 (vw). HRMS (+ESI): *m/z* calcd for [M + H⁺] C₃₈H₄₇N₈O₂Pd⁺ 753.2851, found 753.2911. Anal. Calcd for C₃₈H₄₆N₈O₂Pd: C, 60.59; H, 6.16; N, 14.88. Found: C, 60.42; H, 6.27; N, 14.56.

[PdCl{μ-OC₆H₂(CH₂Pz^{Me2})₂-2,6-Me-4-κN,O,N₂}]₂ 3. Mp > 200 °C. ¹H NMR: (CDCl₃, 400 MHz): δ 7.32 (d, 2H, J(H_AH_B) = 17.2, CH₂), 6.87 (d, 2H, J(H_AH_B) = 14, CH₂), 6.72 (s, 2H, phenyl-CH), 6.54 (s, 2H, phenyl-CH), 5.92 (s, 2H, pyrazole-CH), 5.52 (s, 2H, pyrazole-CH), 5.24 (d, 2H, J(H_AH_B) = 17.6, CH₂), 4.82 (d, 2H, J(H_AH_B) = 14.4, CH₂), 2.73 (s, 6H, pyrazole-CH₃), 2.42 (s, 6H, pyrazole-CH₃), 2.19 (s, 6H, pyrazole-CH₃), 2.06 (s, 6H, pyrazole-CH₃), 0.95 (s, 6H, phenyl-CH₃). ¹³C NMR (CDCl₃, 102.6 MHz): δ 161.6, 153.9, 152.3, 144.3, 142.0, 129.2, 128.9, 127.0, 125.1, 123.0, 108.2, 107.3, 50.6, 49.5, 20.6, 15.9, 13.4, 12.0. FTIR (KBr, cm⁻¹): 3433 (m), 2984 (w), 2919 (m), 2859 (w), 1654 (w), 1612 (w), 1552 (m), 1466 (vs), 1421 (s), 1400 (s), 1351 (m), 1315 (s), 1269 (s), 1206 (m), 1164 (m), 1608 (w), 1036 (w), 984 (w), 934 (vw), 871 (w), 812 (m), 775 (m), 734 (w), 695 (w), 657 (w), 580 (w), 550 (w), 503 (w), 432 (w). HRMS (+ESI): *m/z* calcd for [M + H⁺] C₃₈H₄₇Cl₂N₈O₂Pd⁺: 929.1263, found 929.1235. Anal. Calcd for C₃₈H₄₆Cl₂N₈O₂Pd₂: C, 49.05; H, 4.98; N, 12.04. Found: C, 49.33; H, 5.06; N, 12.16.

[PdCl₂{μ-OC₆H₂(CH₂Pz^{Me2})₂-2,6-Me-4-κN,O,N₂}Pd]₂ 4. Mp > 200 °C. ¹H NMR: (CDCl₃, 400 MHz): δ 7.94 (d, 2H, J(H_AH_B) = 15.6, CH₂), 7.15 (d, 2H, J(H_AH_B) = 18.8, CH₂), 6.79 (s, 2H, phenyl-CH), 5.92 (s, 2H, phenyl-CH), 5.80 (s, 2H, pyrazole-CH), 5.79 (s, 2H,

pyrazole-CH), 5.07 (dd, 4H, J(H_AH_B) = 18.6, CH₂), 2.89 (s, 6H, pyrazole-CH₃), 2.38 (s, 6H, pyrazole-CH₃), 2.07 (s, 6H, pyrazole-CH₃), 2.06 (s, 6H, phenyl-CH₃). ¹³C NMR (CDCl₃, 102.6 MHz): δ 161.2, 149.4, 149.0, 143.6, 142.0, 128.8, 126.7, 126.4, 122.0, 117.5, 107.6, 107.0, 53.1, 52.3, 20.8, 15.1, 13.5, 12.1, 12.0. FTIR (KBr, cm⁻¹): 3129 (vw), 3089 (vw), 2918 (m), 2865 (m), 2663 (vw), 2553 (vw), 1610 (w), 1557 (s), 1464 (vs), 1424 (s), 1395 (s), 1312 (m), 1292 (m), 1226 (s), 1156 (m), 1066 (w), 1037 (w), 944 (w), 864 (w), 804 (m), 735 (m), 658 (vw), 608 (vw), 569 (w), 539 (vw), 508 (w), 442 (w). HRMS (+ESI): *m/z* calcd for [M + H⁺] C₃₈H₄₇Cl₂N₈O₂Pd₂⁺ 929.1263, found 929.1298. Anal. Calcd for C₃₈H₄₆Cl₂N₈O₂Pd₂: C, 49.05; H, 4.98; N, 12.04. Found: C, 49.33; H, 5.06; N, 12.56.

Synthesis of [Pd{OC₆H₂(CH₂Pz^{Me2})₂-2,6-Me-4-κN,O₂}]₂ 2. To a solution of LH (0.113 g, 0.348 mmol) in dry THF was added NaH (0.015 g, 60% in mineral oil, 0.37 mmol), and the solution was stirred for 1 h at room temperature. To this [PdCl₂(COD)] (0.050 g, 0.175 mmol) was added and stirred for 1 h at room temperature. Then, the solvent was removed, and the resulting orange residue was dissolved in dichloromethane (30 mL) and layered with petroleum ether (60 mL). Dark red crystals of complex 2 were obtained over a period of 7 days. The crystals were separated and dried under vacuum (0.062 g, 0.082 mmol, yield: 47%). The identity of 2 synthesized by this method was confirmed by comparing the ¹H NMR spectrum with that of crystals obtained from the above reaction.

Synthesis of [Pd₂Cl₄{μ-HOC₆H₂(CH₂Pz^{Me2})₂-2,6-Me-4-κN,N₂}]₂ 5. To a solution of LH (0.042 g, 0.13 mmol) in dichloromethane (30 mL) was added [PdCl₂(PhCN)₂] (0.050 g, 0.13 mmol). The solution was stirred for 12 h at room temperature and the color of the solution is changed to a yellow-orange. The solution was layered with petroleum ether (60 mL) and yellow colored crystals of complex 5 were formed over a period of 7 days, which were separated and dried under vacuum (0.030 g, 0.030 mmol). Yield: 46%. Mp > 200 °C. ¹H NMR (CDCl₃, 400 MHz): δ 6.83 (s, 4H, phenyl-CH), 6.20 (s, 2H, OH), 5.93 (s, 4H, pyrazole-CH), 5.57 (br s, 8H, CH₂), 2.88 (s, 12H, pyrazole-CH₃), 2.32 (s, 6H, phenyl-CH₃), 2.03 (s, 12H, pyrazole-CH₃). ¹³C NMR (CDCl₃, 102.6 MHz): δ 150.9, 149.9, 144.8, 131.0, 130.3, 122.2, 108.6, 50.6, 20.7, 15.3, 12.6. FTIR (KBr, cm⁻¹): 3341 (br vs), 3136 (m), 2960 (m), 2919 (m), 2863 (m), 1616 (w), 1557 (s), 1477 (vs), 1421 (vs), 1401 (s), 1315 (s), 1291 (m), 1253 (w), 1211 (s), 1147 (m), 1066 (w), 1038 (m), 993 (w), 963 (w), 924 (w), 864 (m), 795 (m), 703 (w), 658 (w), 626 (w), 567 (w), 459 (w). HRMS (+ESI): *m/z* calcd for [M - Cl]⁺ C₃₈H₄₈Cl₃N₈O₂Pd₂⁺ 965.1035, found 965.0999. Anal. Calcd for C₃₈H₄₈Cl₄N₈O₂Pd₂: C, 45.48; H, 4.82; N, 11.17. Found: C, 45.28; H, 4.71; N, 11.07.

General Procedure for Norbornene Polymerization. In a typical norbornene polymerization reaction, 0.001 g (~1 μmol) of crystals of precatalyst (3, 4, or 5) was taken in a 100 mL Schlenk flask and dissolved in toluene. Then, 2.0 g of freshly distilled solid norbornene was added. To this mixture was quickly added MMAO-12 (7 wt % in toluene) with stirring at room temperature. Total volume of the solvent is 10 mL. Precipitate is formed within 30 s and it could not be stirred. The reaction was stopped after 1 min starting from the time at which the MMAO addition is complete by adding MeOH/HCl (v/v = 10/1 mL) mixture. The precipitate was filtered, washed with MeOH several times, and then dried in an oven at 100 °C for 6 h followed by drying under vacuum at 80 °C. In the case of EtAlCl₂ (25 wt % in toluene) as cocatalyst, a thick oily material is formed which became colorless, very soft, gel-like precipitate and dried under vacuum at 80 °C. After drying, it became a very hard one piece of chunk.

Control Experiment with EtAlCl₂. To a toluene solution (10 mL) of norbornene (2.00 g, 21.24 mmol) was quickly added EtAlCl₂ (0.55 mL, 1 mmol, 25 wt % in toluene) with stirring at room temperature. No precipitate or viscous oily materials formed up to 7 min. To this clear solution was then added complex 5 (0.001 g, 1 μmol), and precipitate began to form within 30 s. This confirms that complex 5 is required for polymerization, and it is the precatalyst.

X-ray Crystallography. Suitable single crystals of 1–5 were grown from the solvents mentioned in their respective synthetic

Table 3. Crystallographic Data for Complex 1–5

	1 (C ₇ H ₈) _{1.5}	2	3·(H ₂ O)	4·(CH ₂ Cl) ₂	(S) ₂ ·(H ₂ O) ₄ ·(CH ₂ Cl) ₂
empirical formula	C _{67.50} H ₈₁ N ₁₂ Na ₃ O ₃	C ₃₈ H ₄₆ N ₈ O ₂ Pd	C ₃₈ H ₄₈ Cl ₂ N ₈ O ₃ Pd ₂	C ₄₀ H ₅₀ Cl ₆ N ₈ O ₂ Pd ₅	C ₇₇ H ₁₀₆ Cl ₁₀ N ₁₆ O ₈ Pd ₄
formula weight	1177.41	753.23	948.54	1100.38	2163.87
wavelength (Å)	0.71073	0.71073	0.71073	0.71073	0.71073
temperature (K)	140(2)	298(2)	293(2)	144(2)	293(2)
crystal system	triclinic	monoclinic	orthorhombic	monoclinic	triclinic
space group	$P\bar{1}$	$P2_1/c$	$Ab2$	$P2_1/c$	$P\bar{1}$
<i>a</i> (Å)	14.274(3)	16.158(2)	12.748(3)	20.799(4)	14.9995(15)
<i>b</i> (Å)	15.062(3)	13.574(2)	22.661(5)	10.3719(18)	15.5733(15)
<i>c</i> (Å)	16.748(3)	8.3605(12)	13.926(3)	23.301(4)	22.832(2)
α (degree)	85.850(6)	90	90	90	73.851(5)
β (degree)	67.050(5)	92.729(9)	90	113.901(5)	76.171(5)
γ (degree)	85.501(6)	90	90	90	70.675(5)
volume (Å ³)	3302.1(10)	1831.5(5)	4023.0(14)	459.5(14)	4770.4(8)
<i>Z</i>	2	2	4	4	2
<i>D</i> _{calc} (g cm ⁻³)	1.184	1.366	1.566	1.590	1.506
μ (mm ⁻¹)	0.091	0.551	1.074	1.175	1.079
<i>F</i> (000)	1254	784	1928	2224	2196
θ range (degree)	1.322–25.863	2.864–28.335	1.797–26.466	1.773–24.999	2.755–25.000
limiting indices	–17 ≤ <i>h</i> ≤ 17, –18 ≤ <i>k</i> ≤ 18, –20 ≤ <i>l</i> ≤ 20	–21 ≤ <i>h</i> ≤ 21, –15 ≤ <i>k</i> ≤ 18, –11 ≤ <i>l</i> ≤ 11	–15 ≤ <i>h</i> ≤ 13, –28 ≤ <i>k</i> ≤ 28, –17 ≤ <i>l</i> ≤ 17	–24 ≤ <i>h</i> ≤ 24, –12 ≤ <i>k</i> ≤ 12, –27 ≤ <i>l</i> ≤ 27	–14 ≤ <i>h</i> ≤ 17, –17 ≤ <i>k</i> ≤ 18, –21 ≤ <i>l</i> ≤ 27
total/unique no. of reflns	38932/12234	25486/4545	23678/4048	51405/8088	52034/16744
<i>R</i> _{int}	0.1076	0.1731	0.0364	0.1451	0.0672
data/restr./params.	12234/399/885	4545/0/223	4048/1/241	8088/0/524	16744/0/952
GOF (<i>F</i> ²)	0.944	0.919	1.052	1.016	1.034
<i>R</i> ₁ , <i>wR</i> ₂	0.0770, 0.1838	0.0457, 0.0885	0.0270, 0.0669	0.0554, 0.1152	0.0550, 0.1335
<i>R</i> indices (all data) <i>R</i> ₁ , <i>wR</i> ₂	0.1741, 0.2360	0.1129, 0.1045	0.0334, 0.0699	0.1016, 0.1339	0.0827, 0.1504
largest different peak and hole (e Å ⁻³)	0.392, –0.291	1.006, –0.590	0.400, –0.249	0.710, –0.724	1.248, –2.209

procedures. Single crystal X-ray diffraction data collections were performed using Bruker APEX-II or D8 Venture APEX3 CCD diffractometer with graphite monochromated Mo K α radiation ($\lambda = 0.71073$ Å). The space group for every structure was obtained by XPREP program. The structures were then solved by SIR-92³⁰ or SHELXT³¹ available in WinGX, which successfully located most of the non-hydrogen atoms. Subsequently, least-squares refinements were carried out on F^2 using SHELXL-2018/1 (Sheldrick, 2018)³² to locate the remaining non-hydrogen atoms. Non-hydrogen atoms were refined with anisotropic displacement parameters. All hydrogen atoms were fixed in calculated positions. In the crystal structure of **1**, 1.5 toluene molecules are present in the crystal lattice. One of them is disordered over two positions with occupancy factor of 60 and 40%, and the other toluene has 0.5 occupancy. All of them were refined with DFIX, SADI, and RIGU restraints. In the case of structure (**5**)₂·(H₂O)₄·CH₂Cl₂, all lattice water molecules have been treated as a diffuse contribution to the overall scattering without specific atom positions by SQUEEZE/PLATON.³³ The refinement data for all the structures are given in Table 3.

■ ASSOCIATED CONTENT

📄 Supporting Information

The Supporting Information is available free of charge on the ACS Publications website at DOI: 10.1021/acs.inorgchem.8b00744.

NMR, IR, TGA, powder XRD (PDF)

Accession Codes

CCDC 1831191–1831195 contain the supplementary crystallographic data for this paper. These data can be obtained free of charge via www.ccdc.cam.ac.uk/data_request/cif, or by emailing data_request@ccdc.cam.ac.uk, or by contacting The Cambridge Crystallographic Data Centre, 12 Union Road, Cambridge CB2 1EZ, UK; fax: +44 1223 336033.

■ AUTHOR INFORMATION

Corresponding Author

*E-mail: gmani@chem.iitkgp.ac.in. Phone: +91 3222 282320. Fax: +91 3222 282252.

ORCID

Ganesan Mani: 0000-0002-0782-6484

Notes

The authors declare no competing financial interest.

■ ACKNOWLEDGMENTS

We are thankful to the DST and CSIR (New Delhi, India) for financial support, and DST FIST Level-II grant (No. SR/FST/CSII-026/2013) for 500 MHz NMR machine. We are also thankful to Prof. M. C. Das, Department of Chemistry, IIT-Kharagpur, for TGA and to Vasudevan Subramaniyan for completing one of the X-ray structures.

■ REFERENCES

(1) (a) Janiak, C.; Lassahn, P. G. Metal catalysts for the vinyl polymerization of norbornene. *J. Mol. Catal. A: Chem.* **2001**, *166*, 193–209. (b) Ma, R.; Hou, Y.; Gao, J.; Bao, F. Recent Progress in the Vinylic Polymerization and Copolymerization of Norbornene Catalyzed by Transition Metal Catalysts. *Polym. Rev.* **2009**, *49*, 249–287. (c) Blank, F.; Janiak, C. Metal catalysts for the vinyl/addition polymerization of norbornene. *Coord. Chem. Rev.* **2009**, *253*, 827–861. (d) Yao, Z.-J.; Jin, G.-X. Transition metal complexes based on carboranyl ligands containing N, P, and S donors: Synthesis, reactivity and applications. *Coord. Chem. Rev.* **2013**, *257*, 2522–2535. (2) Tritto, I.; Boggioni, L.; Sacchi, M. C.; Locatelli, P. Cyclic olefin polymerization and relationships between addition and ring opening

metathesis polymerization. *J. Mol. Catal. A: Chem.* **1998**, *133*, 139–150.

(3) (a) Kaminsky, W.; Bark, A.; Arndt, M. New Polymers by homogeneous zirconocene/aluminoxane catalysts. *Makromol. Chem., Macromol. Symp.* **1991**, *47*, 83–93. (b) Arndt, M.; Engehausen, R.; Kaminsky, W.; Zoumis, K. Hydrooligomerization of cycloolefins - a view of the microstructure of polynorbornene. *J. Mol. Catal. A: Chem.* **1995**, *101*, 171–178. (c) Kaminsky, W.; Noll, A. Copolymerization of norbornene and ethene with homogenous zirconocenes/methylaluminoxane catalysts. *Polym. Bull.* **1993**, *31*, 175–182.

(4) Peucker, U.; Heitz, W. Vinylic polymerization by homogeneous chromium(III) catalysts. *Macromol. Rapid Commun.* **1998**, *19*, 159–162.

(5) (a) Goodall, B. L.; McIntosh, L. H., III; Rhodes, L. F. New Catalysts for the polymerization of cyclic olefins. *Macromol. Symp.* **1995**, *89*, 421–432. (b) Sato, Y.; Nakayama, Y.; Yasuda, H. Controlled vinyl-addition-type polymerization of norbornene initiated by several cobalt complexes having substituted terpyridine ligands. *J. Organomet. Chem.* **2004**, *689*, 744–750.

(6) (a) Gao, H.; Guo, W.; Bao, F.; Gui, G.; Zhang, J.; Zhu, F.; Wu, Q. Synthesis, Molecular Structure, and Solution-Dependent Behavior of Nickel Complexes Chelating Anilido–Imine Donors and Their Catalytic Activity toward Olefin Polymerization. *Organometallics* **2004**, *23*, 6273–6280. (b) Huang, Y.-B.; Tang, G.-R.; Jin, G.-Y.; Jin, G.-X. Binuclear Nickel and Copper Complexes with Bridging 2,5-Diamino-1,4-benzoquinonediimines: Synthesis, Structures, and Catalytic Olefin Polymerization. *Organometallics* **2008**, *27*, 259–269. (c) Sujith, S.; Noh, E. K.; Lee, B. Y.; Han, J. W. Synthesis, characterization, and norbornene polymerization of η^3 -benzylnickel(II) complexes of N-heterocyclic carbenes. *J. Organomet. Chem.* **2008**, *693*, 2171–2176. (d) Berding, J.; Lutz, M.; Spek, A. L.; Bouwman, E. Nickel N-heterocyclic carbene complexes in the vinyl polymerization of norbornene. *Appl. Organomet. Chem.* **2011**, *25*, 76–81. (e) Malgas-Enus, R.; Mapolie, S. F. A novel nickel(II) complex based on a cyclam-cored generation-one dendrimeric salicylaldimine ligand and its application as a catalyst precursor in norbornene polymerization: Comparative study with some other first generation DAB-polypropyleneimine metallodendrimers. *Polyhedron* **2012**, *47*, 87–93. (f) Zhang, D.; Zhou, S.; Li, Z.; Wang, Q.; Weng, L. Direct synthesis of cis-dihalo-bis(NHC) complex of nickel(II) and catalytic application in olefin addition polymerization: Effect of halogen co-ligands and density functional theory study. *Dalton Trans.* **2013**, *42*, 12020–12030. (g) Song, H.; Fan, D.; Liu, Y.; Hou, G.; Zi, G. Synthesis, structure, and catalytic activity of nickel complexes with new chiral binaphthyl-based NHC-ligands. *J. Organomet. Chem.* **2013**, *729*, 40–45. (h) Chen, M.; Zou, W.; Cai, Z.; Chen, C. Norbornene homopolymerization and copolymerization with ethylene by phosphinesulfonate nickel catalysts. *Polym. Chem.* **2015**, *6*, 2669–2676. (i) Xu, Y.-M.; Li, K.; Wang, Y.; Deng, W.; Yao, Z.-J. Ligands: Synthesis, Characterization, and Catalytic Activity in Norbornene Polymerization. *Polymers* **2017**, *9*, 105. (j) He, X.; Deng, Y.; Jiang, X.; Wang, Z.; Yang, Y.; Han, Z.; Chen, D. Copolymerization of norbornene and butyl methacrylate at elevated temperatures by a single centre nickel catalyst bearing bulky bis(α -diimine) ligand with strong electron-withdrawing groups. *Polym. Chem.* **2017**, *8*, 2390–2396. (k) Yang, D.; Dong, J.; Wang, B. Homo- and copolymerization of norbornene with tridentate nickel complexes bearing *o*-aryloxide-N-heterocyclic carbene ligands. *Dalton Trans.* **2018**, *47*, 180–189.

(7) (a) Lassahn, P.-G.; Lozan, V.; Janiak, C. Palladium(II) salts containing [PdCl₄]²⁻ and [Pd₂Cl₆]²⁻ ions as pre-catalysts for the vinyl-polymerization of norbornene - evidence for the in situ formation of PdCl₂ as the active species. *Dalton Trans.* **2003**, 927–935. (b) Chemtob, A.; Gilbert, R. G. Catalytic Insertion Polymerization of Norbornene in Miniemulsion. *Macromolecules* **2005**, *38*, 6796–6805. (c) Wang, X.; Liu, S.; Weng, L.-H.; Jin, G.-X. A Trinuclear Silver(I) Functionalized N-Heterocyclic Carbene Complex and Its Use in Transmetalation: Structure and Catalytic Activity for Olefin Polymerization. *Organometallics* **2006**, *25*, 3565–3569. (d) Crosbie, D.; Stubbs, J.; Sundberg, D. Catalytic Emulsion Polymerization of

- Olefins: Ab Initio Polymerization of Norbornene. *Macromolecules* **2007**, *40*, 5743–5749. (e) Crosbie, D.; Stubbs, J.; Sundberg, D. Catalytic Emulsion Polymerization of Olefins: Surfactant Effects in the ab Initio Polymerization of Norbornene. *Macromolecules* **2007**, *40*, 8947–8953. (f) Jung, I. G.; Lee, Y. T.; Choi, S. Y.; Choi, D. S.; Kang, Y. K.; Chung, Y. K. J. Polymerization of 5-norbornene-2-methyl acetate catalyzed by air-stable cationic (η^3 -substituted allyl) palladium complexes of N-heterocyclic carbene. *J. Organomet. Chem.* **2009**, *694*, 297–303. (g) Blank, F.; Scherer, H.; Ruiz, J.; Rodriguez, V.; Janiak, C. Palladium(II) complexes with pentafluorophenyl ligands: structures, C_6F_5 fluxionality by 2D-NMR studies and pre-catalysts for the vinyl addition polymerization of norbornene. *Dalton Trans.* **2010**, *39*, 3609–3619. (h) Blank, F.; Scherer, H.; Janiak, C. Oligomers and soluble polymers from the vinyl polymerization of norbornene and 5-vinyl-2-norbornene with cationic palladium catalysts. *J. Mol. Catal. A: Chem.* **2010**, *330*, 1–9. (i) Blank, F.; Vieth, J.; Ruiz, J.; Rodriguez, V.; Janiak, C. η^5 -Cyclopentadienylpalladium(II) complexes: Synthesis, characterization and use for the vinyl addition polymerization of norbornene and the copolymerization with 5-vinyl-2-norbornene or 5-ethylidene-2-norbornene. *J. Organomet. Chem.* **2011**, *696*, 473–487. (j) Sung, W. Y.; Park, M. H.; Park, J. H.; Eo, M.; Yu, M.; Do, Y.; Lee, M. H. Triarylborane-functionalized polynorbornenes: Direct polymerization and signal amplification in fluoride sensing. *Polymer* **2012**, *53*, 1857–1863. (k) Dang, L.; Song, H.; Wang, B. Synthesis, Structures, and Norbornene Polymerization Behavior of o-Aryloxy-Substituted NHC-Ligated σ , π -Cycloalkenyl Palladium Complexes. *Organometallics* **2014**, *33*, 6812–6818. (l) Zhuang, R.; Liu, H.; Guo, J.; Dong, B.; Zhao, W.; Hu, Y.; Zhang, X. Highly active nickel(II) and palladium(II) complexes bearing N,N,P tridentate ligand for vinyl addition polymerization of norbornene. *Eur. Polym. J.* **2017**, *93*, 358–367.
- (8) (a) Carlini, C.; Giaiacopi, S.; Marchetti, F.; Pinzino, C.; Galletti, A. M. R.; Sbrana, G. Vinyl Polymerization of Norbornene by Bis(salicylaldimine)copper(II)/Methylalumoxane Catalysts. *Organometallics* **2006**, *25*, 3659–3664. (b) Tang, G.; Lin, Y.-J.; Jin, G.-X. Syntheses, structures and catalytic activity of copper(II) complexes with hydroxyindanimine ligands. *J. Organomet. Chem.* **2007**, *692*, 4106–4112. (c) Yao, Z. J.; Li, K.; Zhang, J. Y.; Wang, Y.; Deng, W. Synthesis, characterization and polymerization activity of copper complexes with N, O-chelate ligands. *Inorg. Chim. Acta* **2016**, *450*, 118–123.
- (9) Park, M. H.; Yun, C.; Huh, O. J.; Do, Y.; Yoo, S.; Lee, H. M. Synthesis and hole-transporting properties of vinyl-type polynorbornenes with ethyl ester linked triarylamine side groups. *Synth. Met.* **2010**, *160*, 2000–2007.
- (10) Sun, W.-H.; Yang, H.; Li, Z.; Li, Y. Vinyl Polymerization of Norbornene with Neutral Salicylaldimino Nickel(II) Complexes. *Organometallics* **2003**, *22*, 3678–3683.
- (11) (a) Kong, Y.; Ren, H.; Xu, S.; Song, H.; Liu, B.; Wang, B. Synthesis, Structures, and Norbornene Polymerization Behavior of Bis(aryloxy-N-heterocyclic carbene) Palladium Complexes. *Organometallics* **2009**, *28*, 5934–5940. (b) Kong, Y.; Wen, L.; Song, H.; Xu, S.; Yang, M.; Liu, B.; Wang, B. Synthesis, Structures, and Norbornene Polymerization Behavior of Aryloxy-N-Heterocyclic Carbene Ligated Palladacycles. *Organometallics* **2011**, *30*, 153–159. (c) Li, M.; Song, H.; Wang, B. Synthesis, Structures, and Norbornene Polymerization Behavior of N-Heterocyclic Carbene-Sulfonate-Ligated Palladacycles. *Organometallics* **2015**, *34*, 1969–1977. (d) Yang, D.; Tang, Y.; Song, H.; Wang, B. Synthesis, Structures, and Norbornene Polymerization Behavior of Palladium Complexes Bearing Tridentate o-Aryloxy-N-heterocyclic Carbene Ligands. *Organometallics* **2016**, *35*, 1392–1398.
- (12) Huang, Y.; He, J.; Liu, Z.; Cai, G.; Zhang, S.; Li, X. A highly active chiral (S,S)-bis(oxazoline) Pd(II) alkyl complex/activator catalytic system for vinyl polymerization of norbornene in air and water. *Polym. Chem.* **2017**, *8*, 1217–1222.
- (13) Mathew, J. P.; Reinmuth, A.; Melia, J.; Swords, N.; Risse, W. (η^3 -Allyl)palladium(II) and Palladium(II) Nitrile Catalysts for the Addition Polymerization of Norbornene Derivatives with Functional Groups. *Macromolecules* **1996**, *29*, 2755–2763. (b) Commarieu, B.; Claverie, J. P. Bypassing the lack of reactivity of endo-substituted norbornenes with the catalytic rectification–insertion mechanism. *Chem. Sci.* **2015**, *6*, 2172–2181. (c) Na, Y.; Zhang, D.; Chen, C. Modulating polyolefin properties through the incorporation of nitrogen-containing polar monomers. *Polym. Chem.* **2017**, *8*, 2405–2409. (d) Zhao, M.; Chen, C. Accessing Multiple Catalytically Active States in Redox-Controlled Olefin Polymerization. *ACS Catal.* **2017**, *7*, 7490–7494. (e) Song, G.; Pang, W.; Li, W.; Chen, M.; Chen, C. Phosphine-sulfonate-based nickel catalysts: ethylene polymerization and copolymerization with polar-functionalized norbornenes. *Polym. Chem.* **2017**, *8*, 7400–7405. (f) Chen, M.; Chen, C. Rational Design of High-Performance Phosphine Sulfonate Nickel Catalysts for Ethylene Polymerization and Copolymerization with Polar Monomers. *ACS Catal.* **2017**, *7*, 1308–1312.
- (14) van der Schaaf, P. A.; Wissing, E.; Boersma, J.; Smeets, W. J. J.; Spek, A. L.; van Koten, G. Organozinc Complexes with Monoanionic Chelating Phenolates or 2-Pyridylmethanolates. Molecular Structure of $[Zn(CH_2SiMe_3)\{OCH_2(2-Py)\}]_4$. *Organometallics* **1993**, *12*, 3624–3629.
- (15) Chen, C.-T.; Chang, W.-K.; Sheu, S.-C.; Lee, G.-H.; Ho, T.-I.; Lin, Y.-C.; Wang, Y. Synthesis and Molecular Structure of Novel Zinc(II) Complexes: $[Zn(HL)Cl_2]_n$, $[Zn_2L_2Cl_2]$ and $[Zn_2(\mu-OH)LCl_2]$ [HL = 4-methyl-2,6-bis(pyrazol-1-ylmethyl)phenol]. *J. Chem. Soc., Dalton Trans.* **1991**, 1569–1573.
- (16) Gupta, R.; Mukherjee, S.; Mukherjee, R. Synthesis, magnetism, 1H NMR and redox activity of dicopper(II) complexes having a discrete $\{Cu_2(\mu\text{-phenoxide})_2\}^{2+}$ unit supported by a non-macrocyclic ligand environment. Crystal structure of $[Cu_2(L)_2(OClO_3)_2]$ [HL = 4-methyl-2,6-bis(pyrazol-1-ylmethyl)-phenol]. *J. Chem. Soc., Dalton Trans.* **1999**, 4025–4030.
- (17) Alam, R.; Pal, K.; Shaw, B. K.; Dolai, M.; Pal, N.; Saha, S. K.; Ali, M. Synthesis, structure, catalytic and magnetic properties of a pyrazole based five coordinated di-nuclear cobalt(II) complex. *Polyhedron* **2016**, *106*, 84–91.
- (18) Ghorai, D.; Kumar, S.; Mani, G. Mononuclear, helical binuclear palladium and lithium complexes bearing a new pyrrole-based NNN-pincer ligand: fluxional property. *Dalton Trans.* **2012**, *41*, 9503–9512.
- (19) Guchhait, T.; Barua, B.; Biswas, A.; Basak, B.; Mani, G. Synthesis and structural characterization of silver(I), copper(I) coordination polymers and a helicate palladium(II) complex of dipyrrolylmethane-based dipyrazole ligands: the effect of meso substituents on structural formation. *Dalton Trans.* **2015**, *44*, 9091–9102.
- (20) (a) Hou, Z.; Jia, X.; Fujita, A.; Tezuka, H.; Yamazaki, H.; Wakatsuki, Y. Alkali and Alkaline-Earth Metal Ketyl Complexes: Isolation, Structural Diversity, and Hydrogenation/Protonation Reactions. *Chem. - Eur. J.* **2000**, *6*, 2994–3005. (b) Roy, K.; Wang, C.; Smith, M. D.; Pellechia, P. J.; Shimizu, L. S. Alkali Metal Ions As Probes of Structure and Recognition Properties of Macrocyclic Pyridyl Urea Hosts. *J. Org. Chem.* **2010**, *75*, 5453–5460. (c) Chen, H.-Y.; Mialon, L.; Abboud, K. A.; Miller, S. A. Comparative Study of Lactide Polymerization with Lithium, Sodium, Magnesium, and Calcium Complexes of BHT. *Organometallics* **2012**, *31*, 5252–5261. (d) Boyle, T. J.; Velazquez, A. T.; Yonemoto, D. T.; Alam, T. M.; Moore, C.; Rheingold, A. L. Synthesis and characterization of a family of solvated sodium aryloxy compounds. *Inorg. Chim. Acta* **2013**, *405*, 374–386. (e) Zhang, Q.; Zhang, W.; Wang, S.; Solan, G. A.; Liang, T.; Rajendran, N. M.; Sun, W.-H. Sodium iminoquinolates with cubic and hexagonal prismatic motifs: synthesis, characterization and their catalytic behavior toward the ROP of rac-lactide. *Inorg. Chem. Front.* **2016**, *3*, 1178–1189.
- (21) van der Schaaf, P. A.; Hogerheide, M. P.; Grove, D. M.; Spek, A. L.; van Koten, G. The First Lithium Phenolate with a Trinuclear Structure and the Tetranuclear Product of 1:1 Addition of Lithium Iodide; X-Ray Structures of $[LiOAr]_3$ and $[Li_2(OAr)I]_2$ [OAr = $OC_6H_4(CH_2NMe_2)_2$ -2,6-Me-4]. *J. Chem. Soc., Chem. Commun.* **1992**, 1703–1705.

(22) Yin, C.; Huo, F.; Gao, F.; Guo, J.; Yang, P. 2,6-Bis(3,5-dimethylpyrazol-1-ylmethyl)-4-methylphenol. *Acta Crystallogr., Sect. E: Struct. Rep. Online* **2003**, *59*, o1740–o1741.

(23) k_c (s^{-1}) = $\pi\Delta\nu/\sqrt{2}$, ΔG^\ddagger (kJ mol^{-1}) = $2.303RT_c(10.319 + \log T_c - \log k_c)$. $R = 8.314 \text{ J K}^{-1} \text{ mol}^{-1}$. (a) Calder, I. C.; Garratt, P. J. Unsaturated Monocyclic Compounds. Part XLVIII. A Study by Nuclear Magnetic Resonance of the Energy Barrier for Conformational Interconversion in Annulenes and Dehydro-annulenes. *J. Chem. Soc. B* **1967**, 660–662. (b) Fischer, P.; Fettig, A. Chelate-Type Intramolecular Hydrogen Bridging in 2,4-Diaryl-6-(2-hydroxy-4-methoxyphenyl)-1,3,5-triazines. A Dynamic $^1\text{H}/^{13}\text{C}$ NMR Study. *Magn. Reson. Chem.* **1997**, *35*, 839–844.

(24) (a) Minghetti, G.; Cinelli, M. A.; Bandini, A. L.; Banditelli, G.; Demartin, F.; Manassero, M. Preparation and characterization of palladium(II) and platinum(II) complexes with bis(pyrazolyl)alkanes. crystal and molecular structures of $[\text{Pd}_2(\text{pz})_{22}][\text{BF}_4]_2$ and of $[\text{PdCl}_2\{(\text{CH}_3)_2\text{C}(\text{pz})_2\}]$ (pzH = pyrazole), a new example of a Pd...H-C agostic interaction. *J. Organomet. Chem.* **1986**, *315*, 387–399. (b) Arroyo, N.; Gomez-de la Torre, F.; Jalon, F. A.; Manzano, B. R.; Moreno-Lara, B.; Rodríguez, A. M. New palladium complexes with rigid scorpion-type ligands. Crystal structure of complexes $[\text{Pd}(\eta^3\text{-CH}_3\text{C}_3\text{H}_4)(\text{bpz}^*\text{mPh})](\text{CF}_3\text{SO}_3)$ and $[\text{Pd}(\text{bpz}^*\text{mpy})_2](\text{BF}_4)_2$. bpz*mPh = phenyl-bis(3,5-dimethylpyrazol-1-yl)methane; bpz*mpy = pyridin-2-yl-bis(3,5-dimethylpyrazol-1-yl)methane. *J. Organomet. Chem.* **2000**, *603*, 174–184. (c) Garcia-Anton, J.; Pons, J.; Solans, X.; Font-Bardia, M.; Ros, J. Synthesis of New Pd^{II} Complexes Containing Thioether–Pyrazole Hemilabile Ligands – Structural Analysis by ^1H and ^{13}C NMR Spectroscopy and Crystal Structures of $[\text{PdCl}_2(\text{bddo})]$ and $[\text{Pd}(\text{bddo})](\text{BF}_4)_2$ [bddo = 1,8-Bis(3,5-dimethyl-1-pyrazolyl)-3,6-dithiaoctane]. *Eur. J. Inorg. Chem.* **2002**, *2002*, 3319–3327. (d) Conley, M. P.; Burns, C. T.; Jordan, R. F. Mechanism of Ethylene Oligomerization by a Cationic Palladium(II) Alkyl Complex that Contains a (3,5-Me₂-pyrazolyl)₂CHSi(*p*-tolyl)₃ Ligand. *Organometallics* **2007**, *26*, 6750–6759. (e) Sánchez-Méndez, A.; de Jesús, E.; Flores, J. C.; Gómez-Sal, P. Crystal Structures of Poly(aryl ether) Dendrons with Palladium Scorpionate Complexes at Their Focal Point. *Inorg. Chem.* **2007**, *46*, 4793–4795. (f) John, A.; Shaikh, M. M.; Butcher, R. J.; Ghosh, P. Highly efficient palladium precatalysts of homoscorpionate bispyrazolyl ligands for the more challenging Suzuki–Miyaura cross-coupling of aryl chlorides. *Dalton Trans.* **2010**, *39*, 7353–7363. (g) Sánchez-Méndez, A.; de Jesús, E.; Flores, J. C.; Gómez-Sal, P. Fréchet-Type Pallado-Dendrimers Containing Bis(pyrazolyl)methane Ligands. *Eur. J. Inorg. Chem.* **2010**, *2010*, 141–151. (h) Hallett, A. J.; Adams, C. J.; Anderson, K. M.; Baber, R. A.; Connelly, N. G.; Prime, C. J. Homo- and heterodinuclear complexes of the tetrakis(pyrazolyl)borate ligand. *Dalton Trans.* **2010**, *39*, 5899–5907. (i) Ghorai, D.; Mani, G. Single-Step Substitution of all the α , β -Positions in Pyrrole: Choice of Binuclear versus Multinuclear Complex of the Novel Polydentate Ligand. *Inorg. Chem.* **2014**, *53*, 4117–4129.

(25) Ghorai, D.; Mani, G. Synthesis and structural characterization of Pd(II) complexes containing 2,6-bis[(dimethylamino)methyl]-4-methylphenolate ligand. *Inorg. Chim. Acta* **2011**, *372*, 412–416.

(26) Lai, Y.-C.; Chen, H.-Y.; Hung, W.-C.; Lin, C.-C.; Hong, F.-E. Palladium catalyzed Suzuki cross-coupling reactions using N,O-bidentate ligands. *Tetrahedron* **2005**, *61*, 9484–9489.

(27) Zhang, Y.; Song, G.; Ma, G.; Zhao, J.; Pan, C.-L.; Li, X. 1,3-Dinitroene Pincer Complexes of Palladium and Nickel: Synthesis, Structural Characterizations, and Catalysis. *Organometallics* **2009**, *28*, 3233–3238.

(28) Drew, D.; Doyle, J. R.; Shaver, A. G. Cyclic Diolefin Complexes of Platinum and Palladium. *Inorg. Synth.* **2007**, *28*, 346.

(29) Anderson, G. K.; Lin, M.; Sen, A.; Gretz, E. Bis(benzonitrile)-dichloro Complexes of Palladium and Platinum. *Inorg. Synth.* **2007**, *28*, 60.

(30) Altomare, A.; Cascarano, G.; Giacovazzo, C.; Guagliardi, A. Completion and refinement of crystal structures with SIR92. *J. Appl. Crystallogr.* **1993**, *26*, 343–350.

(31) Sheldrick, G. M. SHELXT – Integrated space-group and crystalstructureDetermination. *Acta Crystallogr., Sect. A: Found. Adv.* **2015**, *71*, 3–8.

(32) Sheldrick, G. M. Crystal structure refinement with SHELXL. *Acta Crystallogr., Sect. C: Struct. Chem.* **2015**, *71*, 3–8.

(33) van der Sluis, P.; Spek, A. L. BYPASS: an effective method for the refinement of crystal structures containing disordered solvent regions. *Acta Crystallogr., Sect. A: Found. Crystallogr.* **1990**, *46*, 194–201.